On the Analysis of FGM Beams: FEM with Innovative Element

M. Zakeri [1, *], A. Modarakar Haghighi [1,2], R. Attarnejad [1]

[1]*School of Civil Engineering, College of Engineering, University of Tehran, Tehran, Iran*
[2]*Centre of Numerical Methods in Engineering, University of Tehran, Tehran, Iran*

ABSTRACT

This paper aims at presenting a new efficient element for free vibration and instability analysis of Axially Functionally Graded Materials (FGMs) non-prismatic beams using Finite Element Method (FEM). Using concept of Basic Displacement Functions (BDFs), two- node element extends to three-node element for obtaining much more exact results using FEM. First, BDFs are introduced and computed using energy method such as unit-dummy load method. Afterward, new efficient shape functions are developed in terms of BDFs during the procedure based on the mechanical behavior of the element in which presented shape functions benefit generality and accuracy from stiffness and force method, respectively. Finally, deriving structural matrices of the beam with respect to new shape functions; free vibration and instability analysis of the FGM beam are studied using finite element method for all types of AFGM beams and the convergence of FEM has been studied. The results from both free vibration and instability analysis are in perfect agreement with those of previously published.

© 2016 IAU, Arak Branch.All rights reserved.

Keywords : Axially functionally graded materials (AFGM); Finite element method (FEM); Basic displacement functions (BDFs); Free vibration; Instability analysis.

1 INTRODUCTION

F UNCTIONALLY graded materials (FGMs) are a new class of advanced composite materials possessing continuous variation of material properties with respect to the spatial coordinates. Unlike laminated composites, which are prone to interfacial stress concentration, leading to delamination and propagation of cracks, FGMs exhibit smooth and gradual vary in material properties. This can be achieved by either continuous change in thickness direction or smooth change of in-plane materials. During the past two decades the idea of FGMs has had a vast range of application in optics, human implants, engine components, turbine blades, and other engineering fields, as same as, received considerable attention by researchers. This is due to their distinguished characteristics such as high thermal resistance and toughness as well as improved strength. Most of researchers have focused on the FG beams while material properties fluctuate along the dimensions of cross-section all together or independently for beam or plate [1-4]. However, a few of these studies deal with FGMs with materials indices varying through the beam's length [5-33].

The majority of researches conducted in this field are concerned with presenting closed-form solutions. For example, Elishakoff et al.[5-24] have applied the semi inverse method in which the closed-form solution of the

_____
*Corresponding author. Tel.: +98 9127935898 ; Fax: +98 2122323705.
E-mail address: mohammad_zakeri@ut.ac.ir (M. Zakeri).

problem is applicable to the particular problems; the semi-inverse method is only useable for the beams with specific required displacement and a physical property such as mass density. Moreover, other physical property which mainly is the modulus of elasticity, is derived through the satisfying the governing differential equation of the problem. Huang and Li [25] have studied free vibration of axially FG beam with non-uniform cross-sectional area for various flexural rigidity and mass density cases by transforming differential equation into Fredholm integral equation. Alsharbagy et al.[26] adopted FEM to investigate the dynamic characteristics of axially FG beam. Singh et al.[27] also probed stability of non-uniform axially FG beam through modeling non-prismatic beams as an assemblage of several uniform segments. Furthermore, Shahba & Rajasekaran [28] employed two different numerical methods to investigate the free vibration and instability analysis of axially functionally graded beam.

Attarnejadet al. [29-32] have analyzed axially FG Euler-Bernoulli and Timoshenko beam using FEM in which new functions, namely Basic Displacement Functions (BDFs) have been introduced. First, a two-node element has been considered. Then, Basic Displacement Functions (BDFs) are defined and derived for this element considering each node. Afterwards, new shape functions are expressed in terms of BDFs and obtained from a mechanical point of view. Finally, structural stiffness and consistent mass matrix are derived and presented static and free vibration analysis of the FG beams using finite element method. In addition, Shahba et al. [33] have used shape functions of the homogeneous uniform beams to analyze free vibration and instability of non-uniform FG beams with different boundary conditions.

The paper is an extension of already published so called Basic Displacement Functions (BDFs) method for derivation of the shape functions in the FE method. The method is applied to non-uniform tapered beams with axially functionally graded material accounting for the property change along the beam. The method leads to improved convergence of the FE method and the extension to3-node BDFs has even better convergence. The development of the BDF method to 3-node functions and elements results much more accurate natural frequencies, which has been validated through several numerical examples. Counting the advantages of the present method; first, combining of stiffness and force method, a new element is developed which benefits its generality from stiffness method and its accuracy from force method; second, applying the new element, static analysis exactly carried out with one or few elements, consequently the time and cost of analysis considerably decreases; also this method considers the possibility of applying with different boundary conditions and attachments, e.g. concentrated mass and spring.

2   NODE BASIC DISPLACEMENT FUNCTION
2.1 BDFs definition

BDFs are mathematical functions derived from fundamental mechanical concepts. For 2-Node element's BDFs, a cantilever beam is considered [34],while for 3-Node element's BDFs, a beam with one free node is considered while its other nodes are clamped. A BDF is defined as nodal displacement of the free node as a result of unit load at distance x; consequently, BDFs for 3-Node beam elements have the following characteristics:

b_{wm} : Vertical displacement of the mth node due to a unit lateral load at distance x when the beam is clamped at the other nodes (Fig. (1a), (1e) and (1c)).

$b_{\theta m}$: Rotation angle of the mth node due to a unit lateral load at distance x when the beam is clamped at other nodes (Fig. (1b), (1d) and (1f)).

b_{um} : Axial displacement of the mth node due to a unit axial load at distance x when the beam is clamped at other nodes (Fig. (1g), (1h) and (1i)).

According to reciprocal theorem, the equivalent definition of BDFs can be defined as follows:

b_{wm} : Vertical displacement of a point at distance x due to a unit vertical load at the mth node when the beam is clamped at the other nodes (Fig. (2a),(2c) and (2e)).

$b_{\theta m}$: Rotation angle of a point at distance x due to a unit load at the mth node when the beam is clamped at the other nodes (Fig. (2b),(2d) and (2f)).

b_{um} : Axial displacement of a point at distance x due to a unit axial load at the mth node when the beam is clamped at the other nodes (Fig. (2g),(2h) and (2i)).
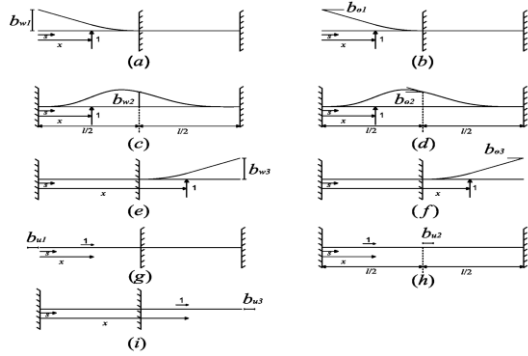
Fig.1
Definition of BDFs: (a) b_{w1} ;(b) $b_{\theta1}$;(c) b_{w2} ;(d) $b_{\theta2}$;(e) b_{w3} ;(f) $b_{\theta3}$ (g) ;b_{u2} (h) ;b_{u2} ;(i) b_{u3}.
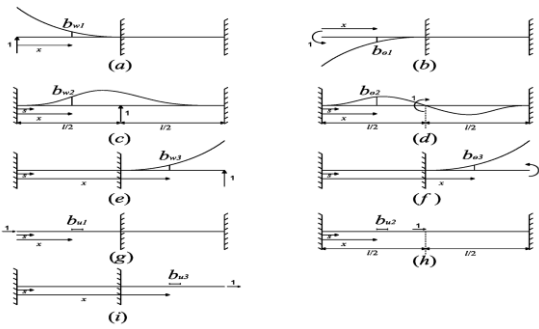
Fig.2
Equivalents to BDFs: (a) b_{w1} ;(b) $b_{\theta1}$;(c) b_{w2} ;(d) $b_{\theta2}$;(e) b_{w3} ;(f) $b_{\theta3}$;(g) b_{u2} ;(h) b_{u2} ;(i) b_{u3}.

2.2 BDFs computation
2.2.1 Node 1 and 3

BDFs for node 1 and 3are obtained using unit load method:

$$b_{w1}(x) = H\left(\frac{l}{2} - x\right) \int_x^{l/2} \frac{s(s-x)}{EI(s)} ds + \operatorname{sgn}\left(\frac{l}{2} - x\right) \int_x^{l/2} \frac{s(s-x)}{EI(s)} \tag{1}$$

$$b_{\theta1}(x) = H\left(\frac{l}{2} - x\right) \int_x^{l/2} \frac{-(s-x)}{EI(s)} ds + \operatorname{sgn}\left(\frac{l}{2} - x\right) \int_x^{l/2} \frac{-(s-x)}{EI(s)} ds \tag{2}$$

$$b_{w3} = H\left(x - \frac{l}{2}\right) \int_{l/2}^x \frac{(l-s)(x-s)}{EI(s)} ds + \operatorname{sgn}\left(x - \frac{l}{2}\right) \int_{l/2}^x \frac{(l-s)(x-s)}{EI(s)} \tag{3}$$

$$b_{\theta3} = H\left(x - \frac{l}{2}\right) \int_{l/2}^x \frac{-(s-x)}{EI(s)} ds + \operatorname{sgn}\left(x - \frac{l}{2}\right) \int_{l/2}^x \frac{-(s-x)}{EI(s)} \tag{4}$$

where:

$$\operatorname{sgn}(x) = \begin{cases} 0 & x < 0, x > 0 \\ \frac{1}{2} & x = 0 \end{cases} \quad , \quad H(x) = \begin{cases} 1 & x > 0 \\ \frac{1}{2} & x = 0 \\ 0 & x < 0 \end{cases}$$

2.2.2 Node 2

For midpoint node, reactions at node 1 are determined according to a unit vertical load at distance x , as shown in Fig. 3:

$$R_1 = \frac{\int\limits_x^l \frac{s(s-x)}{EI(s)}ds \int\limits_0^l \frac{1}{EI(s)}ds - \int\limits_x^l \frac{(s-x)}{EI(s)}ds \int\limits_0^l \frac{s}{EI(s)}ds}{\int\limits_0^l \frac{s^2}{EI(s)}ds \int\limits_0^l \frac{1}{EI(s)}ds - \left(\int\limits_0^l \frac{s}{EI(s)}ds\right)^2}$$

(5a)

$$M_1 = \frac{\int\limits_x^l \frac{s(s-x)}{EI(s)}ds \int\limits_0^l \frac{s}{EI(s)}ds - \int\limits_x^l \frac{(s-x)}{EI(s)}ds \int\limits_0^l \frac{s^2}{EI(s)}ds}{\int\limits_0^l \frac{s^2}{EI(s)}ds \int\limits_0^l \frac{1}{EI(s)}ds - \left(\int\limits_0^l \frac{s}{EI(s)}ds\right)^2}$$

(5b)

From which the moment through the beam, M_s (corresponding to a unit vertical load at distance x) is obtained:

$$M_s = R_1 s - M_1 - H(s-x)(s-x)$$

(6)

Following a similar procedure, support reactions due to a unit vertical load at distance $l/2$ are estimated (Fig. 4):

$$R_1' = \frac{\int\limits_{l/2}^l \frac{s(s-l/2)}{EI(s)}ds \int\limits_0^l \frac{1}{EI(s)}ds - \int\limits_{l/2}^l \frac{(s-l/2)}{EI(s)}ds \int\limits_0^l \frac{s}{EI(s)}ds}{\int\limits_0^l \frac{s^2}{EI(s)}ds \int\limits_0^l \frac{1}{EI(s)}ds - \left(\int\limits_0^l \frac{s}{EI(s)}ds\right)^2}$$

(7a)

$$M_1' = \frac{\int\limits_{l/2}^l \frac{s(s-l/2)}{EI(s)}ds \int\limits_0^l \frac{s}{EI(s)}ds - \int\limits_{l/2}^l \frac{(s-l/2)}{EI(s)}ds \int\limits_0^l \frac{s^2}{EI(s)}ds}{\int\limits_0^l \frac{s^2}{EI(s)}ds \int\limits_0^l \frac{1}{EI(s)}ds - \left(\int\limits_0^l \frac{s}{EI(s)}ds\right)^2}$$

(7b)

From which the moment through the beam, M_s' (corresponding to a unit vertical load at distance $l/2$) is defined as:

$$M_s' = R_1's - M_1' - H(s-\frac{l}{2})\left(s-\frac{l}{2}\right)$$

(8)

The moment reaction corresponding to unit moment at distance $l/2$ could be calculated similarly (Fig. 5):

$$R_1'' = \frac{\int\limits_{l/2}^l \frac{s}{EI(s)}ds \int\limits_0^l \frac{1}{EI(s)}ds - \int\limits_{l/2}^l \frac{1}{EI(s)}ds \int\limits_0^l \frac{s}{EI(s)}ds}{\int\limits_0^l \frac{s^2}{EI(s)}ds \int\limits_0^l \frac{1}{EI(s)}ds - \left(\int\limits_0^l \frac{s}{EI(s)}ds\right)^2}$$

(9a)

$$M_1'' = \frac{\int\limits_{l/2}^l \frac{s}{EI(s)}ds \int\limits_0^l \frac{s}{EI(s)}ds - \int\limits_{l/2}^l \frac{1}{EI(s)}ds \int\limits_0^l \frac{s^2}{EI(s)}ds}{\int\limits_0^l \frac{s^2}{EI(s)}ds \int\limits_0^l \frac{1}{EI(s)}ds - \left(\int\limits_0^l \frac{s}{EI(s)}ds\right)^2}$$

(9b)

From which the moment through the beam, M_s'' (correlated to unit moment at distance x) is derived:

$$M_s^{''} = M_1^{''} - R_1^{''}s + H(s - \frac{l}{2})$$ (10)

Finally, BDFs of mid-point are derived using virtual work principle as follows:

$$b_{w2}(x) = \int_0^l \frac{M_s M_s^{'}}{EI(s)} ds$$ (11)

$$b_{\theta2}(x) = \int_0^l \frac{M_s M_s^{''}}{EI(s)} ds$$ (12)

Similarly, support reaction to a unit longitudinal load at distance x is achieved (Fig. 6):

$$N_1 = \frac{-\int_x^l \frac{1}{EA(s)} ds}{\int_0^l \frac{1}{EA(s)} ds}$$ (13)

Thus axial load through the beam, N_s is evaluated as follows:

$$N_s = N_1 + H(s - x)$$ (14)

Afterward, support reaction due to a unit longitudinal load at distance $l/2$ is calculated according to Fig. 7:

$$N_1' = \frac{-\int_{l/2}^l \frac{1}{EA(s)} ds}{\int_0^l \frac{1}{EA(s)} ds}$$ (15)

Axial load through the beam (deal with a unit longitudinal load at distance x) is obtained:

$$N_s^{'} = N_1^{'} + H(s - \frac{l}{2})$$ (16)

Finally, BDF associated with axial displacement of mid-point is derived as:

$$b_{u2} = \int_0^l \frac{N_s N_s^{'}}{EA(s)} ds$$ (17)
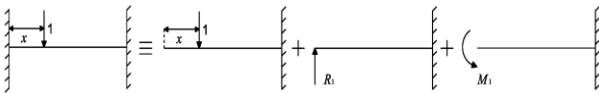
Fig.3
Calculating support reactions of node 1 when a vertical unit load is exerted at distance x.
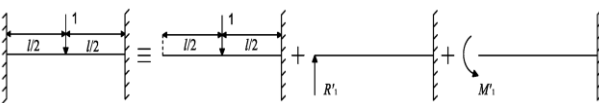
Fig.4
Calculating reactions of node 1 when a vertical unit load is exerted at distance $l/2$.
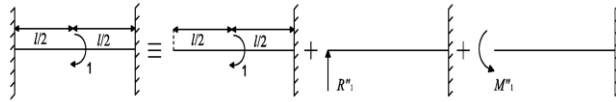
Fig.5
Calculating reaction of node 1 when unit moment is applied at distance *l/2*.
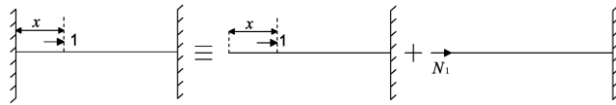
Fig.6
Calculating support reaction of node 1 when an axial unit load is exerted at distance *x*.
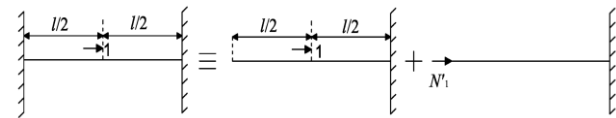
Fig.7
Calculating support reaction of node 1 when an axial unit load is exerted at distance l/2.

2.3 Nodal flexibility matrices

According to the definitions of nodal flexibilities and equivalent definitions of BDFs, nodal flexibility matrices are derived as:

$$
F_{11} = \begin{bmatrix} b_{u1}(0) & 0 & 0 \\ 0 & b_{w1}(0) & b_{\theta 1}(0) \\ 0 & \left.\dfrac{db_{w1}}{dx}\right|_{x=0} & \left.\dfrac{db_{\theta 1}}{dx}\right|_{x=0} \end{bmatrix}
$$

(18a)

$$
F_{22} = \begin{bmatrix} b_{u2}(l/2) & 0 & 0 \\ 0 & b_{w2}(l/2) & b_{\theta 2}(l/2) \\ 0 & \left.\dfrac{db_{w2}}{dx}\right|_{x=l/2} & \left.\dfrac{db_{\theta 2}}{dx}\right|_{x=l/2} \end{bmatrix}
$$

(18b)

$$
F_{33} = \begin{bmatrix} b_{u3}(l) & 0 & 0 \\ 0 & b_{w3}(l) & b_{\theta 3}(l) \\ 0 & \left.\dfrac{db_{w3}}{dx}\right|_{x=l} & \left.\dfrac{db_{\theta 3}}{dx}\right|_{x=l} \end{bmatrix}
$$

(18c)

where subscripts 1, 2 and 3 refer to first, middle and end node of the element. Also, the nodal stiffness matrices are inverses of the nodal flexibility matrices.

3   NEW SHAPE FUNCTIONS

Consider a general tapered FG beam element, which is clamped at first, middle, and end nodes where it is subjected to external loading, such structure can be divided into two structures as shown in Fig.8. In structure (8b), regarding the BDFs definitions, nodal displacement at the point (3) due to external load can be obtained as follows:

$$
\begin{Bmatrix} u_3 \\ w_3 \\ \theta_3 \end{Bmatrix}^b = \int_{l/2}^{l} n(x) \begin{Bmatrix} b_{u3} \\ 0 \\ 0 \end{Bmatrix} dx + \int_{l/2}^{l} q(x) \begin{Bmatrix} 0 \\ b_{w3} \\ b_{\theta 3} \end{Bmatrix} dx
$$

(19)

where u_3, w_3 and θ_3 are the axial deformation, lateral deflection and rotation angle at the point (3), respectively. In structure (8c), nodal displacement at the point (3) can be evaluated by using the flexibility matrix:

$$\begin{Bmatrix} u_3 \\ w_3 \\ \theta_3 \end{Bmatrix}^{(c)} = F_{33} \begin{Bmatrix} N_3 \\ V_3 \\ M_3 \end{Bmatrix} \tag{20}$$

Imposing boundary conditions on the displacement of point (3), the following equations would be resulted:

$$\begin{Bmatrix} u_3 \\ w_3 \\ \theta_3 \end{Bmatrix}^{b} + \begin{Bmatrix} u_3 \\ w_3 \\ \theta_3 \end{Bmatrix}^{c} = \begin{Bmatrix} u_3 \\ w_3 \\ \theta_3 \end{Bmatrix}^{a} = 0 \tag{21}$$

Substituting Eqs. (19) and (20) into Eq. (21), the reactions at the point (3) are obtained:

$$\begin{Bmatrix} N_3 \\ V_3 \\ M_3 \end{Bmatrix} = -K_{33} \left(\int_{l/2}^{l} n(x) \begin{Bmatrix} b_{u3} \\ 0 \\ 0 \end{Bmatrix} dx + \int_{l/2}^{l} q(x) \begin{Bmatrix} 0 \\ b_{w3} \\ b_{\theta3} \end{Bmatrix} dx \right) \tag{22}$$

In the same way, the reactions at point (1) and (2) are derived:

$$\begin{Bmatrix} N_1 \\ V_1 \\ M_1 \end{Bmatrix} = -K_{11} \left(\int_{0}^{l/2} n(x) \begin{Bmatrix} b_{u1} \\ 0 \\ 0 \end{Bmatrix} dx + \int_{0}^{l/2} q(x) \begin{Bmatrix} 0 \\ b_{w1} \\ b_{\theta1} \end{Bmatrix} dx \right) \tag{23}$$

$$\begin{Bmatrix} N_2 \\ V_2 \\ M_2 \end{Bmatrix} = -K_{22} \left(\int_{0}^{l} n(x) \begin{Bmatrix} b_{u2} \\ 0 \\ 0 \end{Bmatrix} dx + \int_{0}^{l} q(x) \begin{Bmatrix} 0 \\ b_{w2} \\ b_{\theta2} \end{Bmatrix} dx \right) \tag{24}$$

Considering the structural analysis, the nodal equivalent forces are negative of the supporting reactions. Hence, Eqs. (22), (23) and (24) could be rewritten according to axial and flexural deformation as follows:

$$\begin{Bmatrix} F_1 \\ F_4 \\ F_7 \end{Bmatrix} = G_a \left(\int_{0}^{l} n(x) b_a dx \right) \tag{25a}$$

$$\begin{Bmatrix} F_2 \\ F_3 \\ F_5 \\ F_6 \\ F_8 \\ F_9 \end{Bmatrix} = G_f \left(\int_{0}^{l} q(x) b_f dx \right) \tag{25b}$$

Here

$$b_a = \{ b_{u1} \quad b_{u2} \quad b_{u3} \}^T$$
$$b_f = \{ b_{w1} \quad b_{\theta1} \quad b_{w2} \quad b_{\theta2} \quad b_{w3} \quad b_{\theta3} \}^T$$

$F_i, i = 1,2,...,6$ are the equivalent nodal forces as shown in Fig. 9, G_a and G_f can be calculated using nodal axial and flexural stiffness matrices, respectively:

$$G_a = \begin{bmatrix} b_{u1}(0) & 0 & 0 \\ 0 & b_{u2}(l/2) & 0 \\ 0 & 0 & b_{u3}(l) \end{bmatrix}^{-1}$$

(26a)

$$G_f = \begin{bmatrix} b_{w1}(0) & b_{\theta1}(0) & 0 & 0 & 0 & 0 \\ \dfrac{db_{w1}}{dx}\bigg|_{x=0} & \dfrac{db_{\theta1}}{dx}\bigg|_{x=0} & 0 & 0 & 0 & 0 \\ 0 & 0 & b_{w2}(l/2) & b_{\theta2}(l/2) & 0 & 0 \\ 0 & 0 & \dfrac{db_{w2}}{dx}\bigg|_{x=l/2} & \dfrac{db_{\theta2}}{dx}\bigg|_{x=l/2} & 0 & 0 \\ 0 & 0 & 0 & 0 & b_{w3}(l) & b_{\theta3}(l) \\ 0 & 0 & 0 & 0 & \dfrac{db_{w3}}{dx}\bigg|_{x=l} & \dfrac{db_{\theta3}}{dx}\bigg|_{x=l} \end{bmatrix}^{-1}$$

(26b)

Axial and lateral shape functions yields, respectively:

$$N_u = b_a^T G_a$$

(27a)

$$N_w = b_f^T G_f$$

(27b)
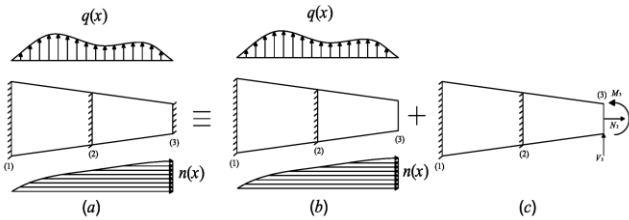
Fig.8
Resolution of 3-node clamped beam by superposition principle.
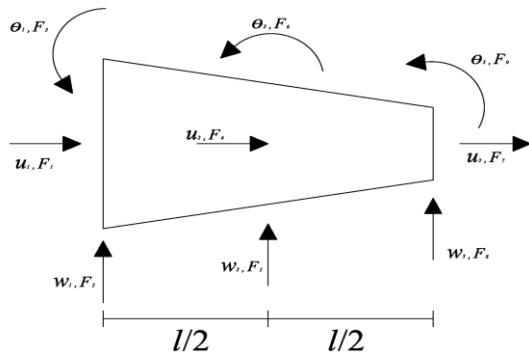
Fig.9
Nodal degree of freedom and positive direction at each node.

3.1 Structural matrices

In order to perform a structural analysis, structural matrices must be computed. Hence, axial and vertical stiffness matrices (K_a, K_f), geometrical matrix (K_g), consistent mass matrices (M_a, M_f) and axial and vertical equivalent nodal forces (F_a, F_f) are evaluated by the following equations:

$$K_a = \int_0^l N_u'^T E(x) A(x) N_u' dx$$

(28a)

$$\mathrm{K_f} = \int_0^l \mathrm{N}_w''^T E(x) I(x) \mathrm{N}_w'' dx \tag{28b}$$

$$\mathrm{K_g} = \int_0^l \mathrm{N}_w'^T P \, \mathrm{N}_w' dx \tag{28c}$$

$$\mathrm{M_a} = \int_0^l \mathrm{N}_u^T \rho(x) A(x) \mathrm{N}_u dx \tag{28d}$$

$$\mathrm{M_f} = \int_0^l \mathrm{N}_w^T \rho(x) A(x) \mathrm{N}_w dx \tag{28e}$$

$$\mathrm{F_a} = \int_0^l n(x) \mathrm{N}_u^T dx \tag{28f}$$

$$\mathrm{F_f} = \int_0^l q(x) \mathrm{N}_w^T dx \tag{28g}$$

In which ($'$) denotes differentiation in respect to x, and subscript a and f are presented as axial and flexural deformation, respectively. N_w and N_u are two vectors representing the shape functions of the beam which correspond to the lateral and axial deformations, respectively, so :

$$w(x) = \{N_{w1} \quad N_{\theta 1} \quad N_{w2} \quad N_{\theta 2} \quad N_{w3} \quad N_{\theta 3}\} \begin{Bmatrix} w_1 \\ \theta_1 \\ w_2 \\ \theta_2 \\ w_3 \\ \theta_3 \end{Bmatrix} \tag{29a}$$

$$u(x) = \{N_{u1} \quad N_{u2} \quad N_{u3}\} \begin{Bmatrix} u_1 \\ u_2 \\ u_3 \end{Bmatrix} \tag{29b}$$

when the shape functions are calculated, the structural matrices and the vectors are presented in terms of BDFs as follows:

$$\mathrm{K_a} = \mathrm{G_a} \left(\int_0^l b_u'^T E(x) A(x) b_u' dx \right) \mathrm{G_a} \tag{30a}$$

$$\mathrm{K_f} = \mathrm{G_f} \left(\int_0^l b_w''^T E(x) I(x) b_w'' dx \right) \mathrm{G_f} \tag{30b}$$

$$\mathrm{K_g} = \mathrm{G_f} \left(\int_0^l b_w'^T P \, b_w' dx \right) \mathrm{G_f} \tag{30c}$$

$$\mathrm{M_a} = \mathrm{G_a} \left(\int_0^l b_u^T \rho(x) A(x) b_u dx \right) \mathrm{G_a} \tag{30d}$$

$$M_f = G_f \left(\int_0^l b_w^T \rho(x) A(x) b_w dx \right) G_f \tag{30e}$$

$$F_a = G_a \left(\int_0^l n(x) b_u^T dx \right) \tag{30f}$$

$$F_f = G_f \left(\int_0^l q(x) b_w^T dx \right) \tag{30g}$$

3.2 Structural analysis

In order to investigate free vibration and instability analyses of beam, eigenvalue of these following equations must be obtained:
   Free longitudinal vibration:

$$K_a^g \phi = \mu_L^2 M_a^g \phi \tag{31}$$

   Free transverse vibration:

$$K_f^g \phi = \mu_T^2 M_f^g \phi \tag{32}$$

   Instability analysis:

$$\left(K_f^g + \lambda K_g^g \right) \phi = 0 \tag{33}$$

   Static analysis:

$$\Delta x = F_a / K_a \tag{34}$$

$$\Delta y = F_f / K_f \tag{35}$$

where μ_L, μ_T are the longitudinal and transverse natural frequencies of beam, respectively and ϕ is the mode shape of the beam. Also, the superscript *g* designates the global structural matrix which is obtained through assembling the elemental matrices and imposing the boundary conditions and λ is eigenvalue in the instability analysis equation. So the critical load can be obtained as:

$$P_{cr} = \lambda P \tag{36}$$

where *P* is the constant compressive load.Therefore, to derive structural matrices of the FG beam, the following step by step procedure is suggested:
   a)   Calculating axial and flexural BDFs for first and end nodes using Eqs.(1-4).
   b)   Computing flexural BDFs for mid-point node using Eqs.(11&12).
   c)   Calculating axial BDFs for mid-point node using Eq.(17).
   d)   Determining G_a and G_f using Eqs.(26a & 26b).
   e)   Derivation of shape functions using Eqs. (27a & 27b).
   f)   Computing the structural matrices using Eqs.(30a-30g).
   In order to elucidate the above step by step procedure, a numerical example is been carried out for a prismatic beam with unit length:

Step (a):

$$b_{u1}(x) = H(0.5-x)\frac{-(2x+1)}{2E_0A_0} + \text{sgn}(0.5-x)\frac{-(2x+1)}{2E_0A_0}$$

$$b_{w1}(x) = H(0.5-x)\frac{(x+1)(2x-1)^2}{24E_0I_0} + \text{sgn}(0.5-x)\frac{(x+1)(2x-1)^2}{24E_0I_0}$$

$$b_{\theta1}(x) = H(0.5-x)\frac{-(2x-1)^2}{8E_0I_0} + \text{sgn}(0.5-x)\frac{-(2x-1)^2}{8E_0I_0}$$

$$b_{u3}(x) = H(0.5-x)\frac{(2x+1)}{2E_0A_0} + \text{sgn}(0.5-x)\frac{(2x+1)}{2E_0A_0}$$

$$b_{w3}(x) = H(x-0.5)\frac{-(x-2)(2x-1)^2}{24E_0I_0} + \text{sgn}(x-0.5)\frac{-(x-2)(2x-1)^2}{24E_0I_0}$$

$$b_{\theta3}(x) = H(x-0.5)\frac{(2x-1)^2}{8E_0I_0} + \text{sgn}(x-0.5)\frac{(2x-1)^2}{8E_0I_0}$$

Step (b & c):

$$b_{u2}(x) = H(0.5-x)\frac{x}{2E_0A_0} + H(x-0.5)\frac{-(2x-1)}{2E_0A_0}$$

$$b_{w2}(x) = H(0.5-x)\frac{(3-4x)x^2}{48E_0I_0} + H(x-0.5)\frac{(4x-1)(x-1)^2}{48E_0I_0}$$

$$b_{\theta2}(x) = H(0.5-x)\frac{x^2(2x-1)^2}{8E_0I_0} + H(x-0.5)\frac{(2x-1)(x-1)^2}{8E_0I_0}$$

Step (d):

$$G_a = E_0A_0\begin{bmatrix} 2 & 0 & 0 \\ & 4 & 0 \\ Sym. & & 2 \end{bmatrix} \qquad G_f = E_0I_0\begin{bmatrix} 96 & 24 & 0 & 0 & 0 & 0 \\ & 8 & 0 & 0 & 0 & 0 \\ & & 192 & 0 & 0 & 0 \\ & & & 16 & 0 & 0 \\ & & & & 96 & -24 \\ Sym. & & & & & 8 \end{bmatrix}$$

Step (e):

$$N_{u1} = H(0.5-x)(1-2x) + \text{sgn}(0.5-x)(1-2x)$$
$$N_{u2} = H(0.5-x)2x + H(x-0.5)(2-2x)$$
$$N_{u3} = H(0.5-x)(2x-1) + \text{sgn}(0.5-x)(2x-1)$$
$$N_{w1} = H(0.5-x)(16x^3 - 12x^2 + 1) + \text{sgn}(0.5-x)(16x^3 - 12x^2 + 1)$$
$$N_{\theta1} = H(0.5-x)(4x^3 - 4x^2 + x) + \text{sgn}(0.5-x)(4x^3 - 4x^2 + x)$$
$$N_{w2} = H(0.5-x)4(3-4x)x^2 + H(x-0.5)(16x^3 - 36x^2 + 24x - 4)$$
$$N_{\theta2} = H(0.5-x)2(2x-1)x^2 + H(x-0.5)(4x^3 - 10x^2 + 8x - 2)$$
$$N_{w3} = H(x-0.5)(-16x^3 + 36x^2 - 24x + 5) + \text{sgn}(x-0.5)(-16x^3 + 36x^2 - 24x + 5)$$
$$N_{\theta3} = H(x-0.5)(4x^3 - 8x^2 + 5x - 1) + \text{sgn}(x-0.5)(4x^3 - 8x^2 + 5x - 1)$$

Step (f) :
All structural matrices have been presented in Appendix A.

4   NUMERICAL EXAMPLES

This section intends to comprehensively study the exactness and convergence of the proposed method in free vibration and instability analysis of the beam by providing illustrative example in which mechanical properties vary along the beam axis followed up exponential functions.

Considering variation of the beam's area, A, moment of inertia, I, modulus of elasticity, E and mass density, ρ as:

$$A = A_0 \left(1 - c\zeta\right), I = I_0 \left(1 - c\zeta\right)^3, \rho = \rho_0 e^\zeta, E = E_0 e^\zeta$$

where $\zeta = x / l$, and l is the entire length of the beam and coefficient c is considered as taper ratio ($0 \leq c < 1$). To do a numerical integration, 10 – point Gauss quadrature rule has been established. To illustrate different boundary conditions, some symbols are utilized: *C, S, F* and *G* stand for Clamped, Simple, Free and Guided boundary conditions, respectively.

The following criterion will help determine *i* sufficient element to hold desirable accuracy:

$$Error = \left| \frac{W_{T(i)} - W_{T(i-1)}}{W_{T(i-1)}} \right|$$

where W_{Ti} implies estimated non-dimensional natural frequency or instability analysis of the beam with respect to *i* element, and $W_{T(i-1)}$ is correlated with $i - 1$ element.

4.1 Static analysis

In what follows, A cantilever axially FG nonuniform beam is considered, which is subjected to constant distributed axial and lateral loadings. This beam is statically analyzed for determination of the tip axial and lateral displacements. The results are given in Table 1.

Table 1
Static analysis of a cantilever axially FG tapered beam subjected to constant distributed axial and lateral loadings.

	Axial displacement of the free end ($\bar{U} = u \dfrac{E_0 A_0}{n_0 l^2}$)		Lateral displacement of the free end ($\bar{W} = w \dfrac{E_0 I_0}{q_0 l^4}$)	
Taper ratio	Present NE=1	FEM NE=500	Present NE=1	FEM NE=500
0.1	0.3787	0.3787	0.1095	0.1095
0.3	0.4040	0.4040	0.1237	0.1237
0.5	0.4362	0.4362	0.1435	0.1435
0.8	0.5105	0.5105	0.1967	0.1967

4.2 Free transverse vibration

Non-dimensional free transverse frequencies of the beam, which is a key parameter in structure design and analysis process, have been calculated by dividing the beam to 5 finite elements. Also, the results are compared with those of Shahba et al. [29] through the Table 2. and Fig. 10.

Table 2
The first three non-dimensional transverse frequencies ($\mu_T = \omega_T \sqrt{\rho_0 A_0 l^4 / E_0 I_0}$) of an axially FG tapered beam.

Taper ratio		S-S		C-C		C-F		C-S	
		Present	[29]	Present	[29]	Present	[29]	Present	[29]
	NE	5	10	5	10	5	10	5	10
C=0.1	μ_{T1}	9.3144	9.3144	21.2898	21.2898	2.6059	2.6060	13.8471	13.8471
	μ_{T2}	37.5388	37.5388	58.6306	58.6306	19.4129	19.4129	46.7576	46.7576
	μ_{T3}	84.4591	84.4591	114.9654	114.9654	57.1918	57.1918	98.3704	98.3704
C=0.3	μ_{T1}	8.3366	8.3366	18.7484	18.7484	2.7083	2.7083	12.7123	12.7123
	μ_{T2}	33.3231	33.3231	51.8608	51.8608	18.1001	18.1001	41.8410	41.8410
	μ_{T3}	74.9813	74.9813	101.8847	101.8847	51.5914	51.5914	87.6699	87.6699
C=0.5	μ_{T1}	7.2448	7.2448	16.0271	16.0271	2.8563	2.8563	11.4426	11.4426
	μ_{T2}	28.8372	28.8372	44.5698	44.5698	16.6882	16.6882	36.5472	36.5472
	μ_{T3}	64.8336	64.8336	87.7671	87.7671	45.6088	45.6088	76.1390	76.1390
C=0.8	μ_{T1}	5.1747	5.1747	11.2653	11.2653	3.2923	3.2923	9.0249	9.0249
	μ_{T2}	21.0856	21.0856	31.6911	31.6911	14.3621	14.3621	27.2088	27.2088
	μ_{T3}	47.1324	47.1324	62.7280	62.7280	35.4046	35.4046	55.798	55.7982
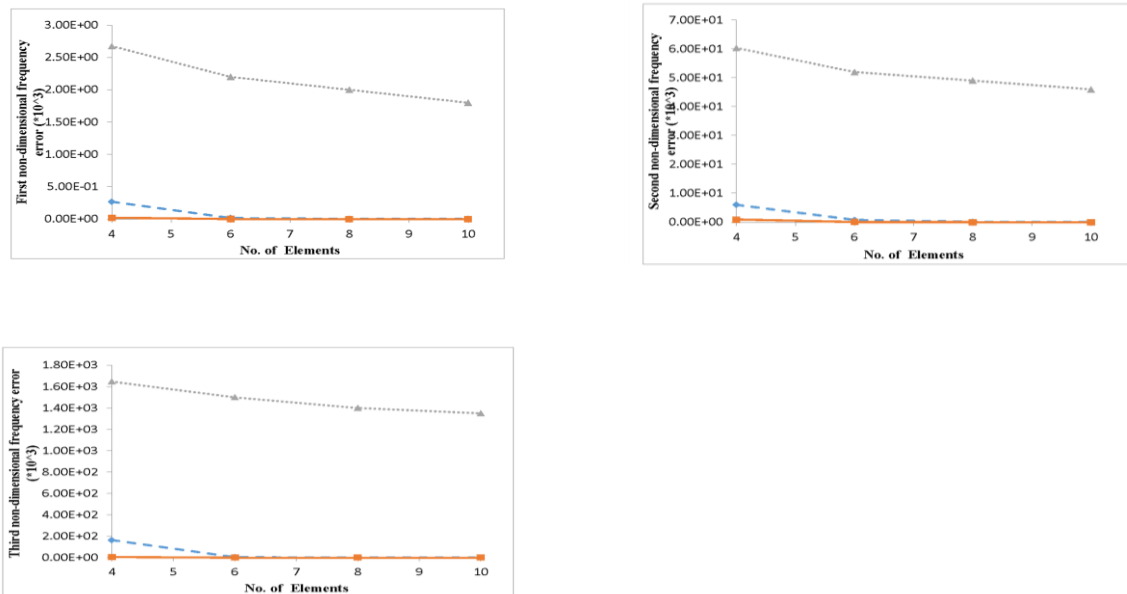
Fig.10
Comparing the effects of three methods' (solid line: 3-node BDFs, Dashed line: 2-node BDFs, Dotted line: P-version FEM) convergence of the free transverse frequency for a cantilever axially graded taper beam ($c = 0.1$).

4.3 Free longitudinal vibration

Dividing the considered beam to 10 finite elements, the first three free longitudinal frequencies have been calculated and the results have been tabulated in Table 3. and Fig. 11 and compared with those obtained by Shahba et al.[29].

Table 3
The first three non-dimensional longitudinal frequencies ($\mu_L = \omega_L \sqrt{\rho_0 l^2 / E_0}$) of an axially FG tapered beam.

Taper ratio	NE	C-C		C-F	
		Present 10	[29] 20	Present 10	[29] 20
c=0.1	μ_{L1}	3.1757	3.1757	1.2988	1.2988
	μ_{L2}	6.3247	6.3247	4.6478	4.6478
	μ_{L3}	9.5228	9.5228	7.8592	7.8592
c=0.3	μ_{L1}	3.1514	3.1514	1.3722	1.3722
	μ_{L2}	6.3123	6.3123	4.6656	4.6656
	μ_{L3}	9.5144	9.5144	7.8698	7.8698
c=0.5	μ_{L1}	3.1120	3.1120	1.4710	1.4710
	μ_{L2}	6.2916	6.2916	4.6983	4.6983
	μ_{L3}	9.5002	9.5005	7.8899	7.8899
c=0.8	μ_{L1}	2.9780	2.9780	1.7168	1.7168
	μ_{L2}	6.2113	6.2113	4.8486	4.8486
	μ_{L3}	9.4427	9.4427	7.9958	7.9958
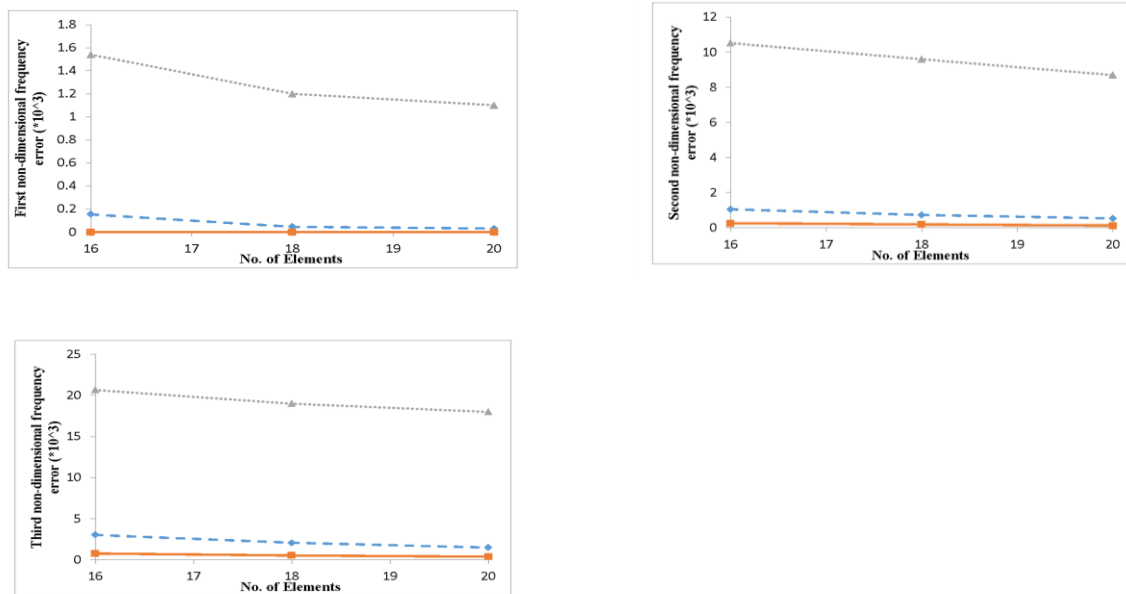
Fig.11
Evaluating the effects of three different methods (solid line: 3-node BDFs, Dashed line: 2-node BDFs, Dotted line: P-version FEM) convergence of the free longitudinal frequency for a clamped-clamped axially graded taper beam ($c = 0.1$).

4.4 Instability analysis

Similarly to the two previous sections, the instability analysis of the beam element when subject to an axial load are presented. The considered beam has been into 10 finite elements and the results are compared to those of Shahbaet al.[29]. Good agreement between the calculated results and those are in the literature has been illustrated through the Table 4. and Fig. 12.

   Moreover, the nine shape functions for different values of taper ratio, c and modulus of elasticity, E are presented in Fig. 13. According to Fig. 13, taper ratio and modulus of elasticity affect perceptibly on the shape functions.

Table 4
Non-dimensional critical load ($\lambda = P_{cr} l^2 / E_0 I_0$) of an axially FG tapered beam-column.

Taper ratio	S-S		C-C		C-F		C-S	
	Present	[29]	Present	[29]	Present	[29]	Present	[29]
NE	5	10	5	10	5	10	5	10
0.1	13.7680	13.7680	55.2302	55.2302	2.9963	2.9963	28.2149	28.2149
0.3	9.9308	9.9308	39.2586	39.2286	2.4919	2.4919	20.1647	20.1647
0.5	6.5134	6.5134	25.1404	25.1404	1.9590	1.9590	13.0091	13.0091
0.8	2.2325	2.2335	7.9289	7.9289	1.0393	1.0393	4.1755	4.1755
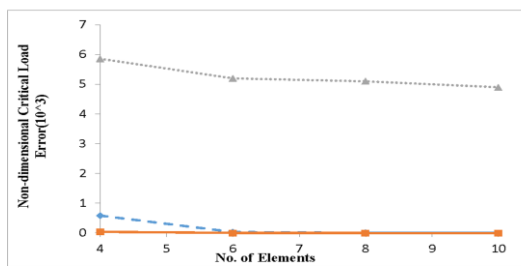
Fig.12
Comparing the effects of three different methods' (solid line: 3-node BDFs, Dashed line: 2-node BDFs, Dotted line: P-version FEM) convergence of the non-dimensional critical load of a clamped-clamped axially graded taper beam ($c = 0.5$).
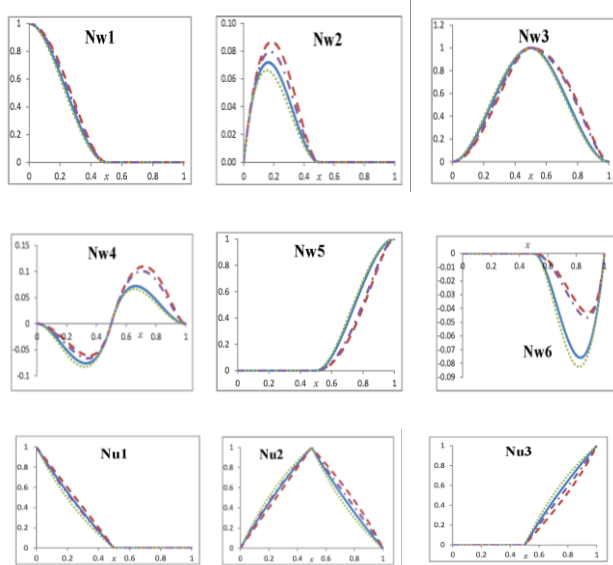
Fig.13
Deriving the shape functions of axially graded FG beams with different mechanical properties(Solid line: $c = 0.2, E = e^x$,Dashed line: $c = 0.8, E = e^x$, Dotted line: $c = 0.2, E = e^{2x}$, Dash-Dot line: $c = 0.2, E = e^{2x}$).

5 CONCLUSIONS

This paper aims at presenting an efficient 3-node element for analysis of FG beams using Finite Element Method (FEM). First, Basic Displacement Functions (BDFs) are defined and then derived using unit-dummy load. Afterwards, new shape functions are expressed in terms of new BDFs and obtained from a mechanical point of view. Finally, structural stiffness and consistent mass matrix are derived and presented free transverse/longitudinal vibration and stability analysis of the considered beams using finite element method. Several numerical examples have been carried out to illustrate the accuracy and economy of the present method and results have been showed through the tables and graphs. The advantages of this new method could be listed as:

1. Any variation for beam's taper ratio and mechanical properties can be considered through the presented method i.e. extended BDFs.
2. Combining of stiffness and force method, a new 3-node element is developed which benefits its generality from stiffness method and its accuracy from force method.
3. New shape functions could be derived on both static and dynamic basis. Although 3-node BDFs were exactly obtained on the basis of static deformation, the new element could be efficiently used in free vibration analysis, as well. But, the new shape functions could be achieved based on dynamic deformation. As a result, their application in dynamic analysis yields more accurate results rather than the application of current static shape functions.
4. Applying the new element, free vibration/instability analysis exactly carried out with few elements rather than existing 2-node BDFs, consequently the time and cost of analysis considerably decreases.
5. BDFs for 3-node element can be extended to BDFs for N-node element in analysis of different beams using finite element method.
6. The concept of 3-node BDFs has proved its competency in different structural applications. Therefore, the authors are extending 3-node BDFs to the other complex and versatile structural elements such as plates and shells.
7. As shown in Table 1. this method is good convergence compared to traditional FEM.
8. This method could be used for solving free vibration of blade rotating beam and modelling of beam in structure.
9. The method is being extended to analysis of plates and shells.
10. This method could be used in computational program for analysis of structures.
11. Results are compared with p-version FEM in Figs .10-12 to show the convergence of this method.

APPENDIX A

$$
K_a = E_0 A_0 \begin{bmatrix} 2 & -2 & 0 \\ & 4 & -2 \\ sym. & & 2 \end{bmatrix}
$$

$$
K_f = E_0 I_0 \begin{bmatrix} 96 & 24 & -96 & 24 & 0 & 0 \\ & 8 & -24 & 4 & 0 & 0 \\ & & 192 & 0 & -96 & 24 \\ & & & 16 & -24 & 4 \\ & & & & 96 & -24 \\ sym. & & & & & 8 \end{bmatrix}
$$

$$
M_a = \rho_0 A_0 \begin{bmatrix} 0.1667 & 0.0833 & 0 \\ & 0.3333 & 0.0833 \\ sym. & & 0.1667 \end{bmatrix}
$$

$$
M_f = \rho_0 A_0 \begin{bmatrix} 0.1857 & 0.0131 & 0.0643 & -0.0077 & 0 & 0 \\ & 0.0012 & 0.0077 & -0.0009 & 0 & 0 \\ & & 0.3714 & 0 & 0.0643 & -0.0077 \\ & & & 0.0024 & 0.0077 & -0.0009 \\ & & & & 0.1857 & -0.0131 \\ sym. & & & & & 0.0012 \end{bmatrix}
$$

REFERENCES

[1]   Chakraborty A., Gopalakrishnan S., Reddy J.N., 2003, A new beam finite element for the analysis of functionally graded materials, *International Journal of Mechanical Sciences* **45**(3): 519-539.
[2]   Carrera E., Brischetto S., Robaldo A., 2008, Variable kinematic model for the analysis of functionally graded material plates, *AIAA Journal* **46**(1): 194-203.
[3]   Giunta G., Belouettar S., Carrera E., 2010, Analysis of FGM beams by means of classical and advanced theories, *Mechanics of Advanced Materials and Structures* **17**(8): 622-635.
[4]   Şimşek M., 2010, Vibration analysis of a functionally graded beam under a moving mass by using different beam theories, *Composite Structures* **92**(4): 904-917.

[5]   Elishakoff I., Becquet R., 2000, Closed-form solutions for natural frequencies for inhomogeneous beams with one sliding support and the other clamped, *Journal of Sound and Vibration* **238**: 540-546.
[6]   Calio I., Elishakoff I., 2005, Closed-form solutions for axially graded beam-columns, *Journal of Sound and Vibration* **280**: 1083-1094.
[7]   Bequet R., Elishakoff I., 2001, Class of analytical closed-form polynomial solutions for clamped-guided inhomogeneous beams, *Chaos, Solitons & Fractals* **12**: 1657-1678.
[8]   Calio I., Elishakoff I., 2004, Closed-form trigonometric solutions for inhomogeneous beam-columns on elastic foundation, *International Journal of Structural Stability and Dynamics* **4**(1):139-146.
[9]   Elishakoff I., Candan S., 2001, Apparently first closed-form solution for vibrating inhomogeneous beams, *International Journal of Solids and Structures* **38**(19): 3411-3441.
[10]   Calio I., Elishakoff I., 2004, Can a trigonometric function serve both as the vibration and the buckling mode of an axially graded structure, *Mechanics Based Design of Structures and Machines* **32**(4): 401-421.
[11]   Elishakoff I., 2001, Inverse buckling problem for inhomogeneous columns, *International Journal of Solids and Structures* **38**(3):457-464.
[12]   Elishakoff I., Becquet R., 2000, Closed-form solutions for natural frequencies for inhomogeneous beams with one sliding support and the other pinned, *Journal of Sound and Vibration* **238**: 529-553.
[13]   Becquet R., Elishakoff I., 2001, Class of analytical closed-form polynomial solutions for guided-pinned inhomogeneous beams, *Chaos, Solitons & Fractals* **12**(8): 1509-1534.
[14]   Guede Z., Elishakoff I., 2001, Apparently the first closed-form solution for inhomogeneous vibrating beams under axial loading, *Proceedings of the Royal Society A* **457**(2007): 623-649.
[15]   Elishakoff I., Guede Z., 2001, A remarkable nature of the effect of boundary conditions on closed-form solutions for vibrating inhomogeneous Euler-Bernoulli beams, *Chaos, Solitons & Fractals* **12**: 659-704.
[16]   Elishakoff I., 2001, Euler's problem revisited: 222 years later, *Meccanica* **36**: 265-272.
[17]   Elishakoff I., Guede Z., 2001, Novel closed-form solutions in buckling of inhomogeneous columns under distributed variable loading, *Chaos, Solitons & Fractals* **12**(6): 1075-1089.
[18]   Elishakoff I., Johnson V., 2005, Apparently the first closed-form solution of vibrating inhomogeneous beam with a tip mass, *Journal of Sound and Vibration* **286**: 1057-1066.
[19]   Elishakoff I., Pentaras D., 2006, Apparently the first closed-form solution of inhomogeneous elastically restrained vibrating beams, *Journal of Sound and Vibration* **298**(1-2): 439-445.
[20]   Wu L., Wang Q.S., Elishakoff I., 2005, Semi-inverse for axially functionally graded beams with an anti-symmetric vibration mode, *Journal of Sound and Vibration* **284**(3-5): 1190-1202.
[21]   Elishakoff I., Perez A., 2005, Design of a polynomially inhomogeneous bar with a tip mass for specied mode shape and natural frequency, *Journal of Sound and Vibration* **287**(4-5): 1004-1012.
[22]   Elishakoff I., 2001, Some unexpected results in vibration of nonhomogeneous beams on elastic foundation, *Chaos, Solitons & Fractals* **12**(12): 2177-2218.
[23]   Guede Z., Elishakoff I., 2001, A fifth-order polynomial that serves as both buckling and vibration mode of an inhomogeneous structure, *Chaos, Solitons & Fractals* **12**(7): 1267-1298.
[24]   Elishakoff I., Guede Z., 2004, Analytical polynomial solutions for vibrating axially graded beams, *Mechanics of Advanced Materials and Structures* **11**(6): 517-533.
[25]   Huang Y., Li X.F.A., 2010, New approach for free vibration of axially functionally graded beams with non-uniform cross-section, *Journal of Sound and Vibration* **329**(11): 2291-2303.
[26]   Alshorbagy A.E., Eltaher M.A., Mahmoud F.F., 2011, Free vibration characteristics of a functionally graded beam by finite element method, *Applied Mathematical Modelling* **35**(1): 412-425.
[27]   Singh K.V., Li G., 2009, Buckling of functionally graded and elastically restrained non-uniform columns, *Composites Part B* **40**(5): 393-403.
[28]   Shahba A., Rajasekaran S., 2012, Free vibration and stability of tapered Euler–Bernoulli beams made of axially functionally graded materials, *Applied Mathematical Modelling* **36**(7): 3094-3111.
[29]   Shahba A., Attarnejad R., Hajilar S., 2013, A mechanical-based solution for axially functionally graded tapered euler-bernoulli beams, *Mechanics of Advanced Materials and Structures* **20**: 696-707.
[30]   Zarrinzadeh H., Attarnejad R., Shahba A., 2012, Free vibration of rotating axially functionally graded tapered beams, *Proceedings of The Institution of Mechanical Engineers Part G-journal of Aerospace Engineering* **226**: 363-379.
[31]   Shahba A., Attarnejad R., Zarrinzadeh H., 2013, Free Vibration Analysis of Centrifugally Stiffened Tapered Functionally Graded Beams, *Mechanics of Advanced Materials and Structures* **20**(5): 331-338.
[32]   Shahba A., Attarnejad R., TavanaieMarvi M., Hajilar S., 2011, Free vibration and stability analysis of axially functionally graded tapered Timoshenko beams with classical and non-classical boundary conditions, *Composites Part B* **42**(4): 801-808.
[33]   Shahba A., Attarnejad R., Hajilara S., 2011, Free vibration and stability of axially functionally graded tapered Euler-Bernoulli beams, *Shock and Vibration* **18**(5): 683-696.
[34]   Attarnejad R., 2010, Basic displacement functions in analysis of nonprismatic beams, *Engineering with Computers* **27**(6): 733-745.